

## On the relation between the maximal LCN and the width of the stochastic layer in a driven pendulum

This article has been downloaded from IOPscience. Please scroll down to see the full text article.

1999 J. Phys. A: Math. Gen. 32 431

(<http://iopscience.iop.org/0305-4470/32/2/016>)

View [the table of contents for this issue](#), or go to the [journal homepage](#) for more

Download details:

IP Address: 171.66.16.105

The article was downloaded on 02/06/2010 at 07:31

Please note that [terms and conditions apply](#).

## On the relation between the maximal LCN and the width of the stochastic layer in a driven pendulum

K Tsiganis, A Anastasiadis† and H Varvoglis

Section of Astrophysics, Astronomy and Mechanics, Department of Physics, University of Thessaloniki, GR-54006 Thessaloniki, Greece

Received 15 June 1998, in final form 21 September 1998

**Abstract.** We examine whether the macroscopically measured diffusion rate in the chaotic region of a time-perturbed classical pendulum depends on the value of the maximal Lyapunov characteristic number,  $\lambda$ . In this respect we calculate the functions  $\lambda(l)$ ,  $w(l)$ ,  $\lambda(\epsilon)$  and  $w(\epsilon)$ , where  $l$  denotes the physical length of the pendulum,  $\epsilon$  the strength of the perturbation and  $w$  the width of the stochastic layer around the separatrix. We find that all these functions follow power laws. In particular, both  $\lambda(l)$  and  $w(l)$  scale as the Lyapunov exponent and the width of the resonance of the unperturbed system, i.e. as  $l^{-1/2}$  and  $l^{3/2}$ , respectively. It follows that the width of the stochastic layer is proportional to  $\lambda^{-3}$  so that, for sufficiently small values of  $l$ , stochastic diffusion is restricted to a thin layer and, therefore, practically does not depend on  $\lambda$ .

### 1. Introduction

In a series of papers by Lecar and co-workers (Soper *et al* 1990, Lecar *et al* 1992a, b, Franklin *et al* 1993, Murison *et al* 1994), numerical evidence was presented on the possible existence of a law pertaining to the motion of asteroids in the outer asteroidal belt. According to these results, the value of the maximal Lyapunov characteristic number (LCN),  $\lambda$ , of an asteroid's trajectory is connected to the time interval ('event time',  $T_E$ ) needed for this asteroid to become a planet crosser, through a relation of the form

$$\log T_E = a + b \log \frac{1}{\lambda}. \quad (1)$$

The maximal LCN is defined as the value at which the function  $\chi(t) = \{\ln[d(t)/d(0)]\}/t$  saturates, where by  $d(t)$  we denote the phase-space distance of two initially nearby trajectories differing by  $d(0)$  at  $t = 0$ .

It is evident that the existence of such a relation implies an anti-correlation between the value of the *Lyapunov time*,  $T_L = 1/\lambda$ , and the *diffusion rate* of the trajectory in action space. Equivalently, it states that the extent of action space that the trajectory can visit within a fixed time interval is an increasing function of  $\lambda$ . Milani and co-workers on the other hand (Milani and Nobili 1992, Milani *et al* 1997) have argued against the concept of a simple relationship between chaos and dynamical lifetime, drawing the attention to the discovery of asteroids with large  $\lambda$  which do not become planet crossers for time intervals several orders of magnitude longer than the 'event time' ( $T_E$ ) estimated through equation (1).

† Present address: Institute of Ionospheric and Space Research, National Observatory of Athens, Palea Penteli, GR-15236, Greece.

Recently, Varvoglis and Anastasiadis (1996) showed that, in the case where transport may be considered as governed by a classical Fokker–Planck diffusion equation and the diffusion space is assumed to be infinite and simply connected, a relation of the form of (1) may be recovered analytically. However, the situation where large-scale transport in action space is inhibited by the existence of some kind of ‘quasi-barriers’, i.e. surviving invariant tori and cantori (for 2D systems) or higher-dimensional geometrical objects (for  $n$ D systems,  $n > 2$ ), is common in Hamiltonian systems (see Shlesinger *et al* 1993, Varvoglis *et al* 1997, Tsiganis *et al* 1998, Barbanis *et al* 1998). If we assume that transport in the presence of ‘quasi-barriers’ can still be described by a Fokker–Planck equation, the existence of a law of the form of (1), i.e. a connection between the *macroscopically* measured diffusion rate to certain dynamical properties of the system, should depend on the topological structure of the diffusion space as well.

Of particular interest would be a dynamical system where trajectories can assume large values of  $\lambda$  and yet remain for a long time in a ‘narrow’ stochastic region. Such behaviour has been observed in asteroidal motion near high-order mean motion resonances in the outer asteroid belt, where Murray and Holman (1997) have shown that equation (1) is violated and the diffusion coefficient is action dependent. We argue that this comes as a result of the complicated topological structure of these phase-space regions, where KAM tori and other ‘quasi-barriers’ can restrict the available phase space. Of course, in Hamiltonian systems with three (or more) degrees of freedom, Arnold diffusion can account for the migration of confined chaotic trajectories in action space, but not within physically meaningful time intervals. However, even if the *sticking* of chaotic trajectories to ‘quasi-barriers’ does not last very long, it is enough to establish different transport properties for different phase-space regions (see also Varvoglis *et al* 1997, Tsiganis *et al* 1998). Since such dynamical systems are rather complex, we decided to use a suitable ‘toy model’ in this paper.

Based on the above considerations we chose to study the ‘classical’ pendulum, perturbed by a time-dependent force of the form  $\epsilon \cos(\theta - \omega t)$ . It is known that in the case where low-order resonances do not overlap the dynamics near a resonance are similar to that of a modulated pendulum (Elskens and Escande 1991). This is also true for simple models describing motion near a mean motion resonance in the asteroid belt under the effect of secular frequencies, as discussed in Morbidelli and Froeschlé (1996). In a more recent work Nesvorný and Morbidelli (1998) present an analytic model of three-body resonances (including Saturn). They show that the averaged Hamiltonian, expressed in resonance variables, can be reduced to that of a simple pendulum and, ignoring the secular terms, is integrable. The same holds for the averaged planar circular restricted three-body problem which is a classic model used for the understanding of the main features of the dynamics near a mean motion resonance. This dynamical system of the perturbed pendulum also models other interesting physical processes, such as the motion of a charged particle in the field of two electrostatic plasma waves, and as such has already been studied extensively (Doveil and Escande 1981, Escande and Doveil 1981, Codaccioni *et al* 1982). In the unperturbed case, the characteristic exponent of the principal unstable periodic trajectory as well as the width of the primary resonance, which gives a natural estimate of transport in action space, depend on the pendulum’s physical length,  $l$ , and can be evaluated analytically (see section 2). The effect of increasing the value of  $l$  is to decrease the positive characteristic exponent,  $\mu^+$ , of the unstable trajectory and to ‘expand’ the phase space in the  $p$ -direction (i.e. to increase the width,  $\Delta p$ , of the primary island). It would be reasonable, then, to expect that the perturbed pendulum would have, at least in some cases, similar properties, i.e. that  $\lambda(l)$  and  $w(l)$  would depend on  $l$  on the same way as, correspondingly,  $\mu^+$  and  $\Delta p$ , where  $w$  denotes the width of the stochastic layer. If this is true, then trajectories within the stochastic layer can obtain large values of  $\lambda$ , while being confined in a thin chaotic region, so

that the diffusion rate does not depend effectively on the value of the maximal LCN.

The ‘natural’ parameters of a classical pendulum are its length,  $l$ , its mass,  $m$ , and the value of the gravitational acceleration,  $g$ . However, by keeping the mass and the acceleration of gravity constant, the equations of motion can be cast in a form depending only on one parameter, the length,  $l$ . If a perturbation is introduced, a second parameter should describe the perturbation strength. In our numerical experiments we examined the dependence of  $\lambda$  in the vicinity of the principal unstable periodic trajectory and the width,  $w$ , of the stochastic layer that develops around the separatrix of the 1:1 resonance, on the values of the strength of the perturbation and the length of the pendulum. In the next section we describe in detail our model. Our numerical results are presented in section 3, and the last section is devoted to a discussion.

## 2. The model

The dynamical system described above is defined by a Hamiltonian of the form,

$$H = H_0 + \epsilon H_1 = \frac{p_\theta^2}{2ml^2} - mgl \cos \theta + \epsilon \sin(\theta - \omega t). \quad (2)$$

In the above equations  $(\theta, p_\theta)$  are the canonical variables and  $\omega$  is the perturbation’s frequency.

### 2.1. The integrable case

The characteristic exponent of the unstable equilibrium point, as well as the width of the resonance of the classical pendulum, can be found in the literature (see e.g. Lichtenberg and Lieberman 1983). For reasons of completeness, however, we decided to include here a brief section on their derivation. The phase space of a simple pendulum defined by  $H_0$  is shown in figure 1. The separatrix, for which  $h_0 = mgl$ , passes through the hyperbolic fixed point at  $(\theta, p_\theta) = (\pi, 0)$ . A stability analysis around this point can be easily performed by solving the variational equations

$$\dot{\xi} = A\xi = (\Omega S)\xi \quad (3)$$

where  $\Omega$  is the unit symplectic matrix and  $S$  is the Hessian matrix of  $H_0$  calculated at the fixed point. The solution of (3) is

$$\xi(t) = C^+ e^{\mu^+ t} + C^- e^{\mu^- t} \quad (4)$$

where  $\mu^+ > 0$  and  $\mu^- < 0$  are the eigenvalues of  $A$  and  $C^\pm$  are constants which depend upon the initial conditions. Thus, the characteristic exponents of the unstable periodic orbit of the integrable system take the values

$$\mu^\pm = \pm \sqrt{g/l} \propto l^{-1/2}. \quad (5)$$

In the integrable case there exists a ‘natural’ measure of the maximum change in momentum,  $p_\theta$ , which is the width of the island of the primary resonance,  $\Delta p$  (see figure 1). This can also be found analytically from equation (2) by setting  $\theta = 0$ ,  $\Delta p = 2p_{\max}$ ,  $H_0 = h_0 = mgl$  and  $\epsilon = 0$ . The solution then yields

$$\Delta p = 4m\sqrt{gl^3} \propto l^{3/2}. \quad (6)$$

Introducing now the nonlinear term, one would like to know (a) whether the value of the maximal LCN,  $\lambda$ , and the width of the stochastic layer,  $w$ , of trajectories in the neighbourhood of the unstable periodic orbit show any scaling with  $\epsilon$  and  $l$ , and (b) whether this scaling has any similarity to the scalings of  $\mu^+$  and  $\Delta p$  of the unperturbed system calculated above.

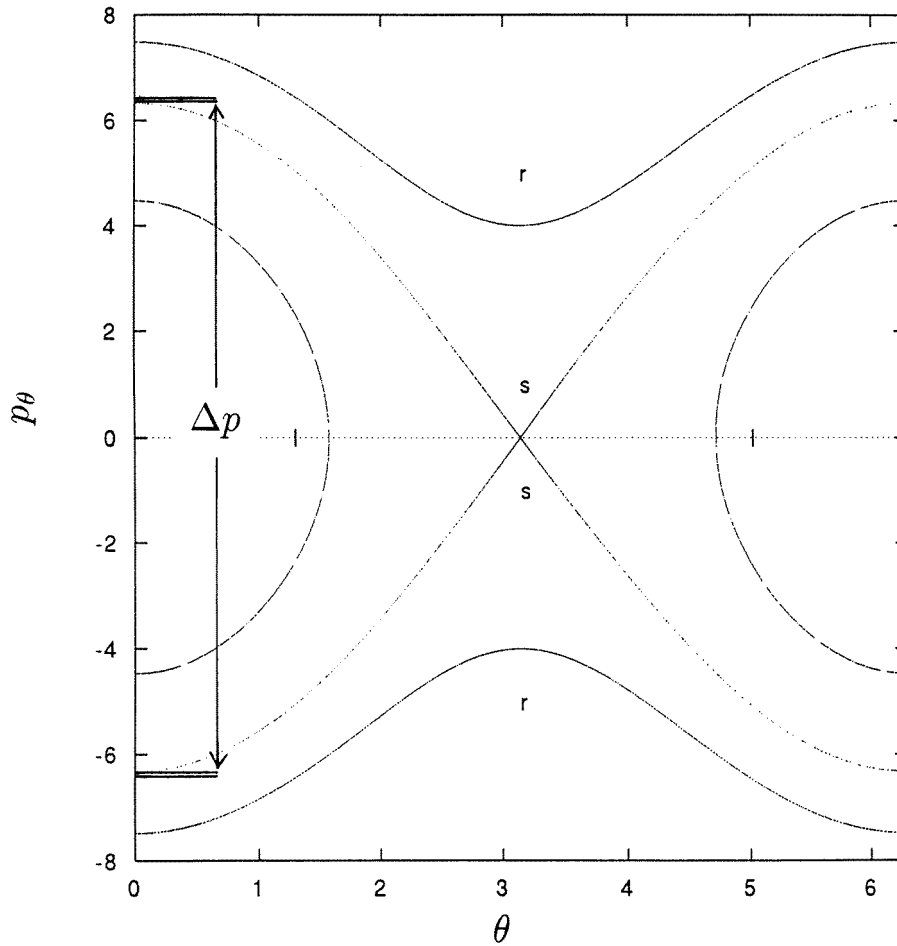


**Figure 1.** The phase space of a classical pendulum. On the left, marked with arrows, the maximum change in momentum,  $\Delta p$ , indicates the width of the island.

## 2.2. The non-integrable case—numerical approach

We consider the non-integrable pendulum whose Hamiltonian is defined by equation (2). Hamilton's equations are then given by

$$\begin{aligned}\dot{\theta} &= \frac{p_{\theta}}{ml^2} \\ \dot{p}_{\theta} &= -mgl \sin(\theta) - \epsilon \cos(\theta - \omega t).\end{aligned}\quad (7)$$

We integrated numerically the above equations for  $g = 10$  and  $m = 1$  using a fourth-order Runge–Kutta algorithm with adaptive step-size control (Press *et al* 1992) with the accuracy level being always set to  $10^{-16}$  (machine accuracy), for initial conditions in the vicinity of the unstable point. We followed a standard numerical technique for the calculation of maximal LCN's (see e.g., Lichtenberg and Lieberman 1983) integrating simultaneously two initially close-by trajectories. Since the variation of the pendulum's length changes the energy of the unperturbed system, we selected the values of  $\epsilon$  in such a way as to represent a certain fraction of  $h_0$  (recall that by  $h_0$  we denote the value of the Hamiltonian at the separatrix of the integrable system).

We studied the system for perturbation strengths in the range  $0.01h_0$ – $0.1h_0$ . The length of the pendulum in all cases took values in the interval  $[1, 10]$ . The canonical equations were integrated over a long time interval, namely  $t = 2 \times 10^5 T$ , where  $T = 2\pi/\omega_0$  and  $\omega_0 = (g/l)^{1/2}$  is the frequency of small oscillations of the unperturbed pendulum. This is necessary for a good estimation of  $\lambda$ , since the presence of secondary islands inside the stochastic region may result in prominent stickiness effects, which would prevent the function  $\chi(t)$  from saturating fast to the value of the maximal LCN.

The perturbation frequency was set to  $\omega/\omega_0 = 1$  for all our experiments. Thus, we are always on the 1:1 resonance; otherwise our results would not be compared consistently. During our study we have also tried different frequency ratios. However, deriving a scaling law for the width of the stochastic layer with the perturbation strength was extremely difficult for these ratios, since at large  $\epsilon$  merging of the stochastic region with neighbouring major subharmonics occurs, something which is not observed in the case  $\omega = \omega_0$  which is presented in this paper.

Adding a perturbation term to the Hamiltonian forces the stable manifold,  $W^S$ , of the homoclinic orbit to intersect with the unstable one,  $W^U$ . The width of the stochastic layer

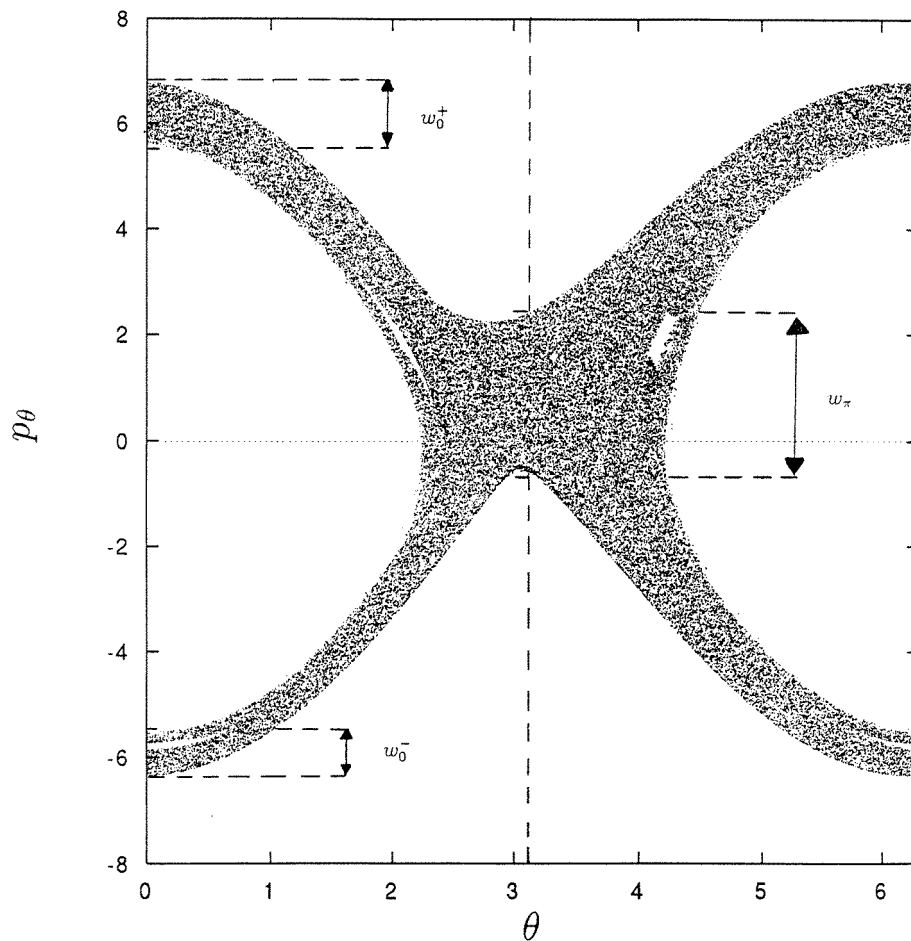


**Figure 2.** Surface of section for  $\epsilon = 0.05h_0$ . The arrows indicate the location in phase,  $\theta$ , at which the  $p$ -width of the stochastic layer is measured, namely  $w_0^+$  and  $w_0^-$  at  $\theta = 0$  and  $w_\pi$  at  $\theta = \pi$ .

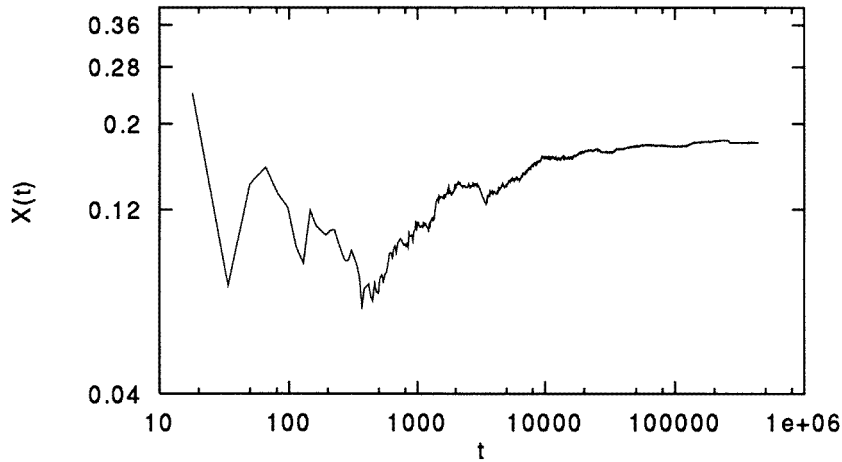


**Figure 3.** Convergence of the function  $\chi(t)$  at the maximal LCN value,  $\lambda$ , after  $t = 2 \times 10^5 T$  for  $\epsilon = 0.05h_0$ .

**Table 1.** The scaling exponent  $\alpha_1$  for different values of  $\epsilon$ .

$\epsilon$	$\alpha$
$0.01h_0$	$0.509 \pm 0.015$
$0.05h_0$	$0.492 \pm 0.018$
$0.10h_0$	$0.522 \pm 0.027$

**Table 2.** The scaling exponents  $\beta_\theta^\pm$  for different  $\epsilon$ .

$\epsilon$	$\beta_0^+$	$\beta_0^-$	$\beta_\pi$
$0.01h_0$	$1.495 \pm 0.024$	$1.468 \pm 0.043$	$1.500 \pm 0.013$
$0.05h_0$	$1.514 \pm 0.049$	$1.541 \pm 0.059$	$1.500 \pm 0.010$
$0.10h_0$	$1.454 \pm 0.052$	$1.555 \pm 0.067$	$1.498 \pm 0.007$

**Table 3.** The scaling exponent  $c_1$  for different values of  $l$ .

$l$	$c_1$
1.0	$0.758 \pm 0.051$
2.0	$0.765 \pm 0.076$
3.0	$0.751 \pm 0.096$
5.0	$0.766 \pm 0.049$
7.0	$0.752 \pm 0.067$
10.0	$0.773 \pm 0.067$

is then proportional to the distance between the two manifolds which is of  $O(\epsilon)$ , as can be found by evaluating the Melnikov function (see e.g. Wiggins 1990). This result is not valid for all values of  $\epsilon$ . In particular, for the numerical results presented here, where  $\epsilon > 10^{-2}$ , we believe that higher-order effects (i.e. merging of the homoclinic layer with neighbouring subharmonics) are not entirely negligible. Thus, an analytic derivation of the exact relation between the width of the stochastic region and  $\epsilon$  is by no means straightforward.

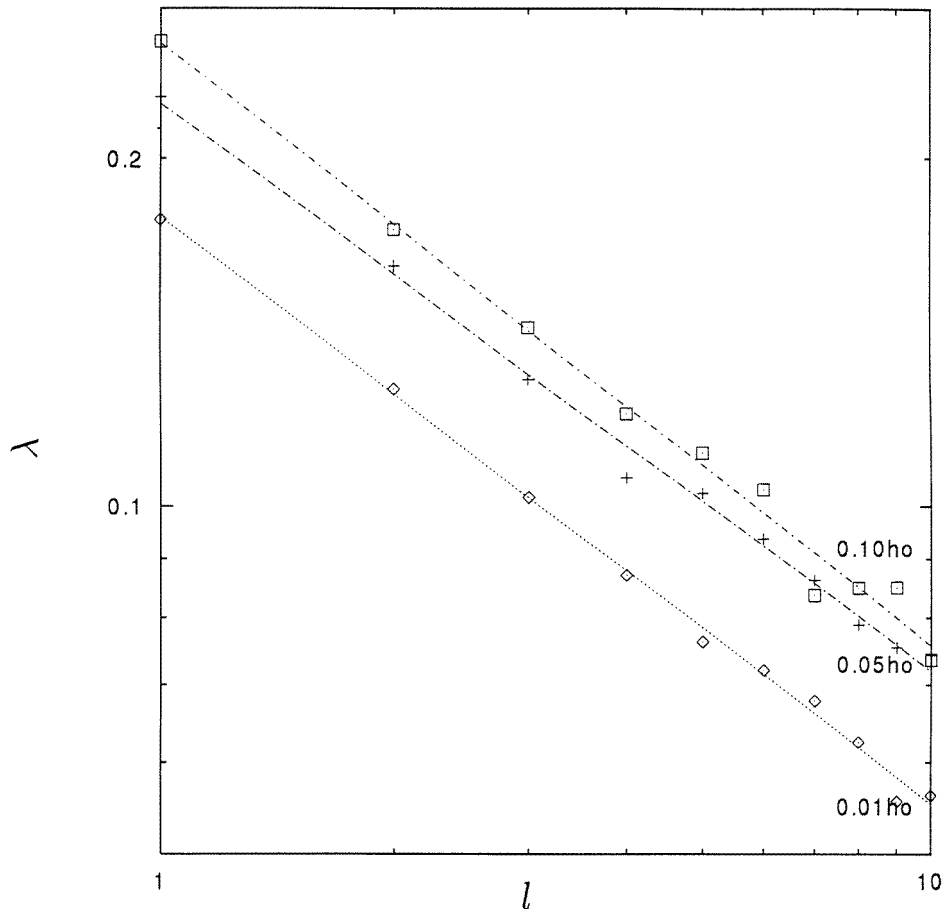


**Figure 4.** Variation of  $\lambda$  with  $l$ . The three different lines correspond to three different perturbation strengths as marked on the graph. All of them indicate a power law with index  $\alpha_1 \approx 0.5$ .

### 3. Numerical Results

In figure 2 a surface of section plot is presented for the case  $\epsilon = 0.05h_0$  and  $l = 1$ . The corresponding  $(\chi, t)$  plot is given in figure 3. As  $\epsilon$  increases, the stochastic layer around the separatrix of the 1:1 resonance becomes thicker. The maximal LCN is also a slightly increasing function of  $\epsilon$ , something that should be expected, since  $\lambda$  is a measure of the system's stochasticity, which is enhanced as  $\epsilon$  is increased. The exact scaling of  $\lambda$  with  $\epsilon$  is examined later in this section.

One of the goals of this paper is to investigate the dependence of  $\lambda$  on the value of  $l$ . Figure 4 shows, in logarithmic scale, the variation of  $\lambda$  as a function of  $l$  for three different values of  $\epsilon = 0.01h_0, 0.05h_0$  and  $0.1h_0$ . It is clear from the plot that the maximal LCN decreases as  $l$  increases, following a power law,

$$\lambda = \alpha_0 l^{-\alpha_1} \quad (8)$$

with  $\alpha_{0,1} > 0$ . The values of  $\alpha_1$  were calculated through a least squares fitting method and are presented in table 1, along with their errors, estimated at a 90% significance level (a method of statistical analysis used throughout the paper). The interesting point is that the value of



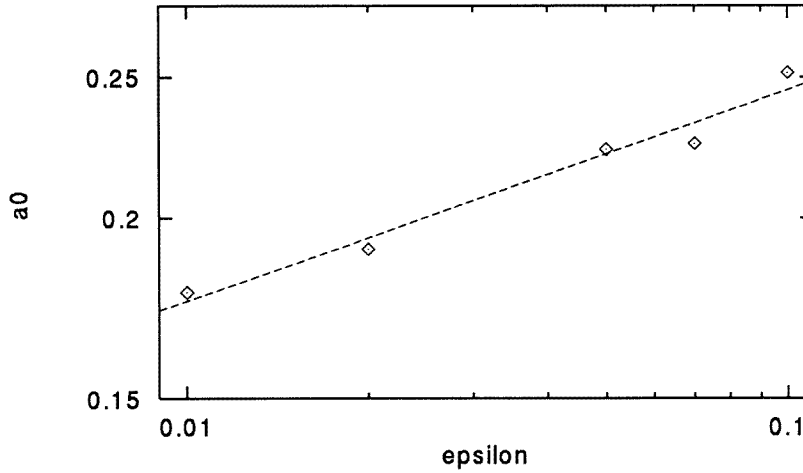


**Figure 5.** Variation of the coefficient  $\alpha_0$ , equation (8), with  $\epsilon$ . A power-law behaviour is again observed.

$\alpha_1$  is equal, up to the numerical accuracy of our results, to the value  $\alpha_1 = 0.5$  obtained for the unperturbed system, in equation (5). For the sake of completeness we examined the dependence of  $\lambda$  on  $\epsilon$  as well. Figure 5 is a plot of the corresponding values of  $\alpha_0$  for different values of  $\epsilon$ . We see that  $\alpha_0$  scales with the value of the perturbation as

$$\alpha_0 = \text{const } \epsilon^\gamma \quad (9)$$

where  $\gamma = 0.146 \pm 0.025$ . We see that the relative value of the estimation error is, in this case, rather large, due to the fact that for large values of  $l$  there are secondary islands that affect the accuracy of the calculations. To obtain a better value  $\gamma$  we focused on the  $l = 1$  case, for which we found  $\gamma = 0.1677 \pm 0.0220$ . Therefore we adopted the value  $\gamma = \frac{1}{6}$ . It is now easy to conclude from equations (8) and (9) that  $\lambda(l, \epsilon)$  can be estimated through the relation

$$\lambda = \text{const } l^{-1/2} \epsilon^{1/6}. \quad (10)$$

Now, as far as the width of the stochastic layer is concerned, it is clear from the surface of section plot that we cannot define a *unique* measure of it, since the width of the layer is a function of the phase angle. For this reason we define the width  $w_\pi = p_{\theta, \max} - p_{\theta, \min}$  at  $\theta = \pi$  and, in a similar way, the widths  $w_0^+ = p_{\theta, \max}^+ - p_{\theta, \min}^+$ ,  $w_0^- = \|p_{\theta, \max}^- - p_{\theta, \min}^-\|$  at  $\theta = 0$ , where the sign + denotes the upper part of the stochastic layer (i.e. positive values of  $p_\theta$ ) and the sign - the lower (i.e. negative values of  $p_\theta$ , see figure 2). Figure 6 shows  $(w_0^\pm, l)$  plots for the three different values of  $\epsilon$  used in our calculations. From this figure and the corresponding table 2 it is evident that *all* three widths ( $w_0^+$ ,  $w_0^-$  and  $w_\pi$ ) follow power laws of the form

$$w_i \propto l^{\beta_i} \quad (i = 0, \pi) \quad (11)$$

where  $\beta_0^\pm$  and  $\beta_\pi$  denote the scaling exponents for  $w_0^\pm$  and  $w_\pi$  respectively. In this case, also, it is remarkable that all the  $\beta$ -values are, up to our numerical accuracy, equal to 1.5. We recall that this is the exponent of the power law giving the ‘natural’ width (the width of the island,  $\Delta p$ ) of the primary resonance of the integrable system, as a function of the pendulum’s length (see equation 6). In what follows, for reasons of notational simplicity, we are using the symbol  $w_0$  in order to denote  $w_0^+$ . It should be emphasized that the derived relations for  $w_0$  are valid for all widths  $w_0^+$ ,  $w_0^-$  and  $w_\pi$ .

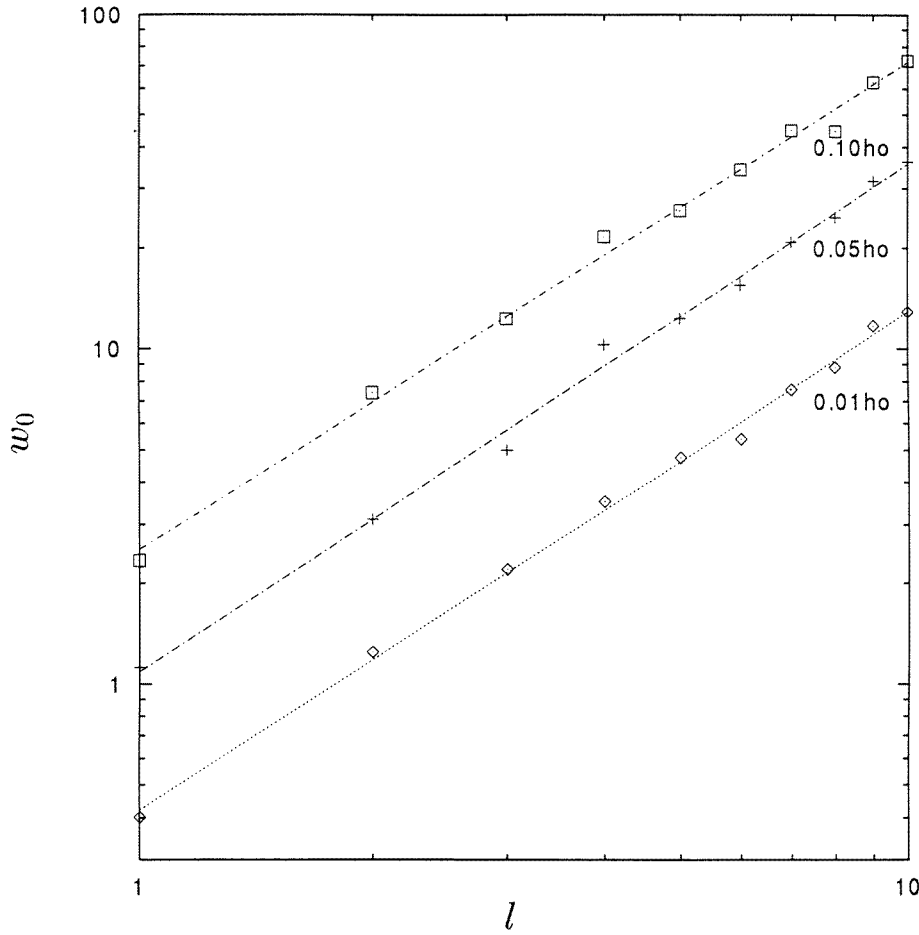


**Figure 6.** Variation of  $w_0$  with  $l$  for three different values of the perturbation strength. All of them show a power-law behaviour of an index  $\beta_0 \approx 1.5$ .

As in the case of the maximal LCN, we also investigated the dependence of the width of the layer on  $\epsilon$  for constant  $l$ . In figure 7 we present a plot of  $w_0$  versus  $\epsilon$  for three different values of  $l$ , namely  $l = 1, 5$  and  $10$ . Since the graph is a straight line in logarithmic scale, the functional dependence of  $w_0$  on  $\epsilon$  is a power law

$$w_0 = c_0 \epsilon^{c_1} \tag{12}$$

where  $c_1$  has a value equal, up to the numerical accuracy of our results, to  $\frac{3}{4}$  as can be seen in table 3. Figure 8 is a plot of the corresponding values of  $c_0$  for the same values of  $l$  as in table 3. We see that  $c_0$  scales with the length of the pendulum as

$$c_0 = \text{const } l^{1.514 \pm 0.037} \tag{13}$$

where the exponent of  $l$  is practically the same as in table 2, i.e.  $\frac{3}{2}$ . It is now easy to conclude, from equations (11)–(13), that the width of the stochastic layer can be estimated through

$$w_0 = \text{const}(l\sqrt{\epsilon})^{3/2} \tag{14}$$

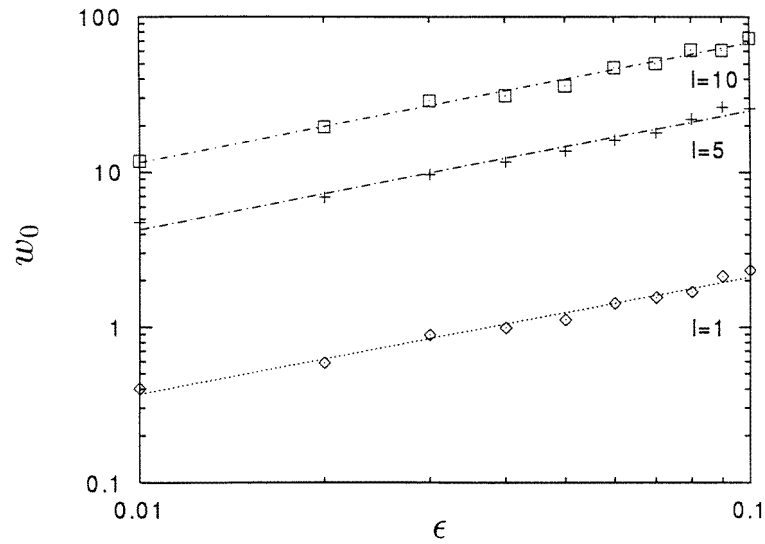


**Figure 7.** Variation of  $w_0$  with  $\epsilon$ . The three curves represent three different values of  $l$ , as marked on the graph. The power-law index is the same for all of them, namely  $c_1 \approx \frac{3}{4}$ .

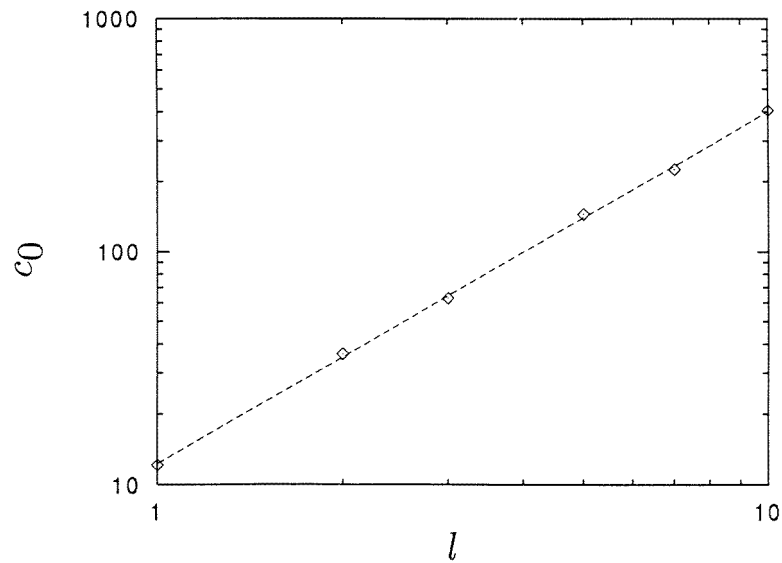


**Figure 8.** Variation of the coefficient  $c_0$ , equation (12), with  $l$ . The power law observed has an index  $\approx 1.5$ .

#### 4. Discussion

The main purpose of this paper was to study transport in the action space of a model non-integrable Hamiltonian system for the particular case where the stochastic region may not be considered as being infinite and simply connected. The motivation was that in the opposite case numerical (Murison *et al* 1994) as well as theoretical (Varvoglis and Anastasiadis 1996) considerations show that the ‘crossing time’ of a particular region of action space is directly

related to the Lyapunov time (i.e. the inverse of the maximal LCN).

From our numerical experiments we have found that, in the simple dynamical system of the classical pendulum selected for study, the value,  $\lambda$ , of the maximal LCN in the neighbourhood of the unstable periodic trajectory as well as the width,  $w$ , of the stochastic layer around the separatrix follow power laws with respect to the physical length,  $l$ , of the pendulum and the strength,  $\epsilon$ , of the perturbation. In particular, for the case of the 1:1 resonance presented in the previous section,  $\lambda$  is a *decreasing* function,

$$\lambda \propto l^{-1/2}$$

while  $w$  is an *increasing* function

$$w \propto l^{3/2}$$

of  $l$ .

Therefore, in the case of a periodically driven pendulum the width of the stochastic layer is inversely proportional to the cube of the maximal LCN and  $l$  may be selected in such a way, as to result in a 'narrow' stochastic layer from which trajectories cannot escape, although characterised by large maximal LCN's. One then may think of higher-dimensional systems, where the presence of 'quasi-barriers' (as defined in this paper) may restrict trajectories for very long times in certain regions of phase space, making the macroscopically measured diffusion rate practically independent of the value of  $\lambda$ . This effect has been discussed recently by Lecar (1996), as well as by Murray and Holman (1997), for the case of the outer asteroid belt and it may explain the conflicting results of Murison *et al* (1994), on one hand, and Milani and Nobili (1992) on the other.

As far as the relation of  $\lambda$  and  $w$  to the perturbation strength is concerned, we have shown that there is a power-law dependence of the form,

$$\lambda \propto \epsilon^{1/6}$$

and

$$w \propto \epsilon^{3/4}.$$

The above results hold for the case of  $\omega = \omega_0$  presented in this paper. As already mentioned in section 2, we also examined other frequency ratios during our study. For these cases the functional dependence of  $w$  and  $\lambda$  on the perturbation strength,  $\epsilon$ , is not clear, since at large  $\epsilon$ 's merging of the stochastic layer with major subharmonics occurs. This effect prevents us from fitting scaling laws for this range of  $\epsilon$ , although it is clear that both  $\lambda(\epsilon)$  and  $w(\epsilon)$  are increasing functions of  $\epsilon$ . Moreover,  $\lambda(l)$  is again a decreasing function of  $l$ , while  $w(l)$  is an increasing one, so that the anticorrelation between the maximal LCN and the width of the stochastic layer holds.

### Acknowledgments

The authors would like to thank Dr S Ichtiaroglou for many stimulating discussions and Professor G Contopoulos and Dr H Islikier for their useful comments on the first draft of the paper. This work was completed while KT was under a Greek State Scholarships Foundation (SSF) grant. KT and AA would like to acknowledge financial support by the PENED-95 programme no 1857 of the Greek General Secretariat of Research and Technology.

### References

Barbanis B, Varvoglis H and Vozikis Ch 1998 *Astron. Astrophys.* submitted

- Codaccioni J P, Doveil F and Escande D F 1982 *Phys. Rev. Lett.* **49** 1879–83
- Doveil F and Escande D F 1981 *Phys. Lett. A* **84** 399–403
- Elskens Y and Escande D F 1991 *Nonlinearity* **4** 615–67
- Escande D F and Doveil F 1981 *Phys. Lett. A* **83** 307–10
- Franklin F, Lecar M and Murison M 1993 *Astron. J.* **105** 2336–43
- Lecar M, Franklin F and Murison M 1992 *Astron. J.* **104** 1230–6
- Lecar M, Franklin F and Soper P 1992 *Icarus* **96** 234–50
- Lecar M 1996 *Celest. Mech. Dyn. Astron.* **64** 163–6
- Lichtenberg A J and Lieberman M A 1983 *Regular and Stochastic Motion* (New York: Springer)
- Milani A and Nobili A M 1992 *Nature* **357** 569–71
- Milani A, Nobili A M and Knezevic Z 1997 *Icarus* **125** 13–31
- Morbidelli A and Froeschlé 1996 *Celest. Mech. Dyn. Astron.* **63** 227–39
- Murison M A, Lecar M and Franklin F 1994 *Astron. J.* **108** 2323–9
- Murray N and Holman M 1997 *Astron. J.* **114** 1246–59
- Nesvorný D and Morbidelli A 1998 *Celest. Mech. Dyn. Astron.* in press
- Press W H, Teukolsky S A, Vetterling W T and Flannery B P 1992 *Numerical Recipes in Fortran—The Art of Scientific Computing* 2nd edn (Cambridge: Cambridge University Press)
- Shlesinger M F, Zaslavsky G M and Klafter J 1993 *Nature* **363** 31
- Soper P, Franklin F and Lecar M 1990 *Icarus* **87** 265–84
- Tsiganis K, Anastasiadis A and Varvoglis H 1998 *J. Phys. A: Math. Gen.* submitted
- Varvoglis H and Anastasiadis A 1996 *Astron. J.* **111** 1718–20
- Varvoglis H, Vozikis Ch and Barbanis B 1997 *The Dynamical Behaviour of Our Planetary System* ed J Henrard and R Dvorak (Dordrecht: Kluwer) p 232
- Wiggin S 1990 *Introduction to Applied Nonlinear Dynamical Systems and Chaos* (New York: Springer)